Theor. Appl. Climatol. 78, 79–96 (2004)
DOI 10.1007/s00704-004-0045-8

Theoretical and Applied Climatology
Printed in Austria

Centro de Previsão de Tempo e Estudos Climaticos, CPTEC/INPE, Cachoeira Paulista, São Paulo, Brazil

Interdecadal variability and trends of rainfall across the Amazon basin

J. A. Marengo

With 7 Figures

Received November 28, 2002; revised June 26, 2003; accepted July 24, 2003
Published online April 27, 2004

Summary

An analysis of decadal and long-term patterns of rainfall has been carried out using a combination of raingauge and gridded rainfall datasets, for the entire Amazon basin and for its northern and southern sub-basins. The study covers the period 1929–98. Rainfall variability and variations in circulation and sea surface temperature fields have been analysed in more detail for the period 1950–98. Negative rainfall trends were identified for the entire Amazon basin, while at the regional level there is a negative trend in northern Amazonia and positive trend in southern Amazonia. Decadal time scale variations in rainfall have been discovered, with periods of relatively drier and wetter conditions, with different behaviour in northern and southern Amazonia. Spectral analyses show decadal time scale variations in southern Amazonia, while northern Amazonia exhibits both interannual and decadal scale variations. Shifts in the rainfall regime in both sections of the Amazon basin were identified as occurring in the mid-1940s and 1970s. After 1975–76, northern Amazonia received less rainfall than before 1975. Changes in the circulation and oceanic fields after 1975 suggest an important role of the warming of the tropical central and eastern Pacific on the decreasing rainfall in northern Amazonia, due to more frequent and intense El Niño events during the relatively dry period 1975–98.

1. Introduction

The variability of rainfall in the Amazon basin at decadal or longer time scales is the result of many complicated interactions. Unravelling these interactions to identify and understand the causes of this variability is hampered by the lack of adequate and continuous climate records throughout the basin. The instrumental record of surface hydrometeorological and upper-air variables in this region is fragmentary: the sparse observations are often inaccurate, are irregularly spaced, and there are very few climate records going back as far as the beginning of the 20th Century. To produce a consistent, long sequence of climatological fields the observations must be blended with model simulations such as the reanalyses, produced by major numerical simulation centres: the National Centers for Environmental Predictions (NCEP), the European Centre for Medium Range Weather Forecasts (ECMWF), and the National Aeronautics and Space Administration-Data Assimilation Office (NASA/DAO) (see reviews by NRC, 1998; Kalnay et al., 1996; and Zhou and Lau, 2001).

Observational studies based on time series of rainfall and river streamflow data (Gentry and Lopez-Parodi, 1980; Rocha et al., 1989; Chu et al., 1994; Dias de Paiva and Clarke, 1995; Marengo et al., 1998; Dettinger et al., 2000a, b; IPCC, 2001; Matsuyama et al., 2002), or reanalyses data (Zhou and Lau, 2001; Costa and Foley,

1999; Curtis and Hastenrath, 1999; Chen et al., 2001) have produced conflicting results, showing both positive and negative trends of rainfall and river streamflow series. For instance, studies by Costa and Foley (1999) have detected tendencies for decreasing moisture convergence into the Amazon Basin during the 1979–98 period, while Curtis and Hastenrath (1999) used the same datasets and methodologies to find a positive trend when analyzing the 1950–99 period. The different tendencies may be in part due to the length of different time series, the spatial data coverage, the use of gridded or station data, or due to the circulation features simulated by the reanalysis in regions where assimilated observations are scarce.

On an interannual time scale, previous studies have documented some association between rainfall deficiency in the Amazon basin and the occurrence of El Niño (Richey et al., 1989; Marengo, 1992; Meggers, 1994; Uvo et al., 1998; Fu et al., 1999, 2001; Liebmann and Marengo, 2001; Botta et al., 2002; and Foley et al., 2002; Ronchail et al., 2002). In that sense, some of these studies have shown that rainfall in northern Amazonia is sensitive to the presence of circulation anomalies associated with strong El Niño or La Niña events. These anomalies are typified by lower than average rainfall and drought with consequently low river levels; examples are the strong El Niño years, 1925 and 1983, and more recently the strong El Niño event in 1998. With the exception of Botta et al. (1992) and Foley et al. (2002), all the studies referred to above used observed raingauge data. Botta et al. and Foley et al. used the Climate Research Unit (CRU) gridded dataset, and found a 3–4 year peak in Amazonian rainfall which was related to the variability in El Niño. They also found a 24–28 year oscillation which has been discussed previously by Marengo and Nobre (2001), and Zhou and Lau (2001), and is indicative of a decadal mode of variability.

The modes of variability on decadal time scales for the Pacific and Atlantic Oceans have been linked to variations of rainfall in regions in northern South America, including Amazonia and Northeast Brazil (Wagner, 1996; Nobre and Shukla, 1996; Robertson and Mechoso, 1998; Dettinger et al., 2000a; and Zhou and Lau, 2001). Zhang et al. (1997) and Mantua et al. (1997) identify a relatively warm period in the Pacific which started in 1976 and is thought to have ended in 2000. This period had more intense and frequent El Niño events compared to the period before 1975. In southern Brazil and northern Argentina, recent studies (Barros, personal communication) have detected increased rainfall and river discharge in the region since the mid-1970s; these increases are linked to changes in the regional circulation, i.e. the southward displacement of the subtropical Atlantic high. On the other hand the tropical Atlantic exhibits decadal variation in the meridional shifts in the position of the Atlantic Intertropical Convergence Zone (ITCZ), as a consequence of the SST contrast between the tropical North and South Atlantic, affecting decadal variations of rainfall in Northeast Brazil and possibly northern Amazonia (Rao et al., 1996; Nobre and Shukla, 1996; Wagner, 1996).

On longer time scales, Costa and Foley (1999) have used the NCEP reanalyses to identify trends in the regional atmospheric circulation showing a statistically significant, decreasing trend in the moisture transport both into and out to the Amazon basin for the 1979–96 period. Furthermore, Curtis and Hastenrath (1999) identified a statistically significant upward trend of lower tropospheric moisture convergence and water vapour transport over Amazonia using the same global reanalyses and methodology, but for the 1958–97 period. This latter result is in agreement with the increased trends in moisture convergence over the whole Amazon region-Atlantic sector as derived by NCEP and NASA/DAO reanalises of the Amazon region as suggested by Chen et al. (2001, 2003), Hastenrath (2001), and Zhou and Lau (2001).

The present study explores the associations of rainfall variability in the whole Amazon basin and its northern and southern sub-basins with decadal and long-term variability patterns identified in the Pacific (the climate shift in the mid-1940s and 1970s), and tropical Atlantic (changes in the moisture transport into the Amazon basin and the latitudinal position of the ITCZ). The major objectives are to investigate patterns of decadal scale variability and trends in the large scale circulation patterns in the Amazon basin, and their associations with shifts in the rainfall regime in the entire basin and its sub-basins.

A combination of circulation fields derived from the NCEP global reanalyses, as well as rainfall observations from raingauge stations in Amazonia and from different gridded rainfall datasets, has been used as a way to investigate and explain tendencies of circulation and the impacts on the rainfall regime across the Amazon basin.

2. Data and methodology

2.1 Rainfall

For this study we have considered monthly rainfall data from almost 300 stations covering the entire Brazilian Amazon for the period 1929–99, drawing from a variety of sources (Fig. 1a, b):

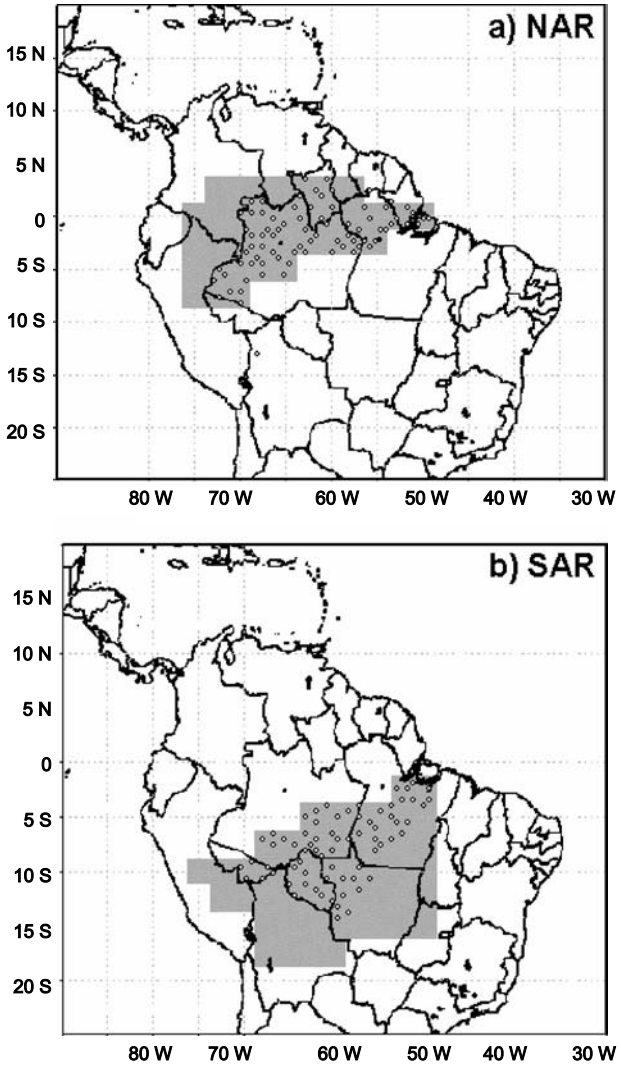

Fig. 1. Location of rainfall stations in the Amazon basin. (**a**) Northern Amazon region, (**b**) Southern Amazon region. Dots represent the location of the stations

ANEEL (Brazilian Agency for Electric Energy), INMET (Brazilian National Institute of Meteorology), CPTEC (Center for Weather Forecasts and Climate Studies), also station data from the GHCN (Global Historical Climatology Network, Vose et al., 1992). In addition we used gridded data from the CRU 0.5°–0.5° lat-long (Climate Research Unit, New et al., 2000), and the CMAP 2.5° lat-long dataset (Xie and Arkin, 1997, 1998). The rainfall station data starts mostly during the 1940s, and with 70% of the total of the station records going back in time to the late 1970s and 40% of the total going back to the late 1920s (mostly from ANEEL, INMET and GHCN). After the early 1950s there is less missing data, so indices after that decade are more representative.

Main basin rainfall is calculated for the entire basin and sub-basins (domains shown in Fig. 1a, b) with a weighted average applied to the gauged data; the same procedure was applied to the gridded data. Some of the gridded products (CMAP, CRU) used interpolation techniques to fill gaps in the gauge coverage. For instance, in the CRU dataset the rainfall station data were interpolated as a function of latitude, longitude and elevation using thin-plate splines. The accuracy of the interpolation was assessed (New et al., 1999) using cross-validation and by comparisons with other climatologies.

Indices representing regional aspects of rainfall in the basin have been implemented by Marengo (1992): NAR (Northern Amazonian Rainfall) and SAR (Southern Amazonia Rainfall) were constructed to represent rainfall regimes in the northern and southern sections of the basin. These, with their domain and the rainfall stations used from each region, are shown in Fig. 1a and b. NAR's domain includes northern and central Amazonia including the mouth of the River Amazon, and shows the season of maximum rainfall: March–April. SAR's domain includes the southern part of the basin, and shows the peak of the rainy season in January–April and a pronounced minimum rainfall during June–August. In both series, observed rainfall totals were seasonalised from September to August, and then mean and standard deviation were calculated. The NAR and SAR rainfall indices are expressed as absolute values (in mm) and also as departures normalised by the standard deviation. These

indices are updated and upgraded to include more stations and extending their time coverage to 1929–98 (the original indices by Marengo (1992) were constructed for the period 1947–87).

From the nearly 300 stations initially available for this study, 164 stations showing data from 1929 were used, with few gaps in the records. An integration of NAR and SAR yields an all-Amazon rainfall index. The new NAR and SAR indices now include 78 and 86 stations, respectively. For comparison with NAR, SAR and the all-Amazon rainfall, indices for the same sub-basins were derived from the above mentioned gridded datasets (NCEP, CRU, CMAP).

Using the CRU dataset we have derived rainfall anomaly maps for South America for decades with relatively drier and wetter conditions, in support of the decadal scale rainfall analyses identified by the NAR and SAR indices and the circulation fields.

2.2 Atmospheric and oceanic datasets

SST and circulation anomaly fields were used to investigate changes in global and regional anomalies in the surface conditions and near surface circulation over tropical oceans. The SST fields were provided by NCEP (Reynolds and Smith, 1994), and the sea level pressure, and 850 hPa zonal and meridional winds were extracted from the NCEP reanalyses (Kalnay et al., 1996). In addition, integrated precipitable water from 1000 to 300 hPa was also calculated from the NCEP reanalyses. The period used is 1950–99 and the data is compiled on a 2.5° latitude/longitude grid for the 30° N–30° S domains.

2.3 Correlation analysis

Correlation coefficients between rainfall anomalies in northern and southern Amazonia and various oceanic and atmospheric fields were calculated for the 1950–98, 1950–75 and 1976–98 periods (see Section 3 for the choice of these periods). Since the peak of the rainy season in northern Amazonia occurs in March–May, we have correlated the NAR with oceanic and atmospheric fields in December, January, February and March. The best correlations were identified during January. For Southern Amazonia, where the peak of the rainy season is in January–March, we have identified the month with the best correlation between SAR and atmospheric and oceanic fields as November. The correlation coefficients were tested for significance at the five percent level for the entire tropical Atlantic and Pacific oceans.

3. Results

The average Amazon basin rainfall of 8.1 mm day^{-1} introduced by Chen et al. (2001, 2003) seems to be unrealistically high when compared to our all-Amazon rainfall mean of 5.9 mm day^{-1}, and also with other estimates of observed mean rainfall from observations and gridded datasets in the Amazon Basin: 5.5 mm day^{-1} (Russell and Miller, 1990), 6.2 mm day^{-1} (Vorosmarty et al., 1989), 5.9 mm day^{-1} (Matsuyama et al., 1992), 7.9 mm day^{-1} (Marengo et al., 1994), 5.0 mm day^{-1} (Xie and Arkin, 1998), 5.9 mm day^{-1} (Costa and Foley, 1998), 5.6 mm day^{-1} (Zeng, 1999), 5.9 mm day^{-1} from the CRU dataset, and 5.8 mm day^{-1} from the NCEP reanalyses.

3.1 Year-to-year and decadal variability and trends of rainfall in Amazonia

From the time series in Fig. 2a, our raingauge based estimates of rainfall as well as those areal indices derived from other different datasets for the entire Amazon basin show a weak positive trend, but from the Mann-Kendall test this tendency is not statistically significant (Fig. 2a). The CRU and our all-Amazon rainfall show similar weak positive trends, while the NCEP reanalyses rainfall shows large positive trends after the beginning of the 1960s.

The rainfall fields from the NCEP reanalyses show a region with relatively low rainfall in central Amazonia, as well as an overestimation along the eastern flank of the Andes. This bias is related to the deficiency of the spectral representation of the orography and the associated circulation. Moreover, the spurious precipitation anomaly in this region was also found by Stern and Miyakoda (1995) and by Marengo et al. (2003) using global climate models; they mention the Gibbs error associated with truncation of steep orography as a possible cause. The CMAP and GHCN trend is too short but these

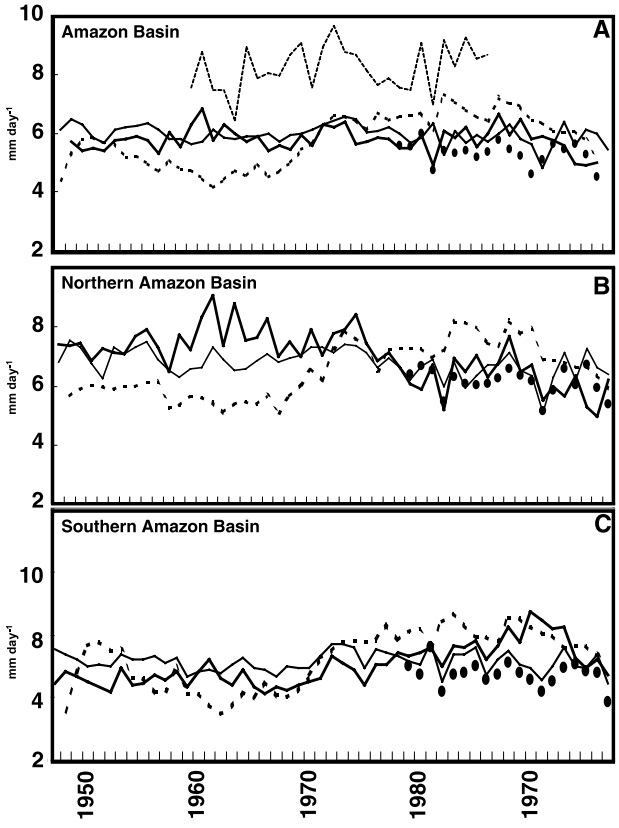

Fig. 2. Rainfall indices for the Amazon basin from different data sources: Gauge rainfall (full lines), CMAP (thin line with circles), NCEP reanalyses (broken line with squares), GHCN (thin broken lines), and CRU (thin line with circles). (**A**) Global Amazonia, (**B**) Northern Amazonia, (**C**) Southern Amazonia. The periods are from September to August, from 1949/50 to 1998/99 for the gauge rainfall CRU and NCEP reanalysis, from 1979/80 to 1998/99 for the CMAP and from 1960/61–88/89 for the GHCN. Units are mm day^{-1}

still show weak positive trends. From the raingauge and gridded datasets, the interannual variability linked to the strong El Niño in 1983, 1987 and 1998 is reflected in reduced rainfall in the basin. Figure 2 shows different trends in the different datasets, and besides the CRU and the raingauge-based rainfall indices (going back from the late 1940s to the late 1990s), the GHCN and CMAP datasets have records of less than 30 years long. Recent studies by Chen at al. (2003) show that the GHCN dataset shows interdecadal variations and a positive trend since the middle 1950s to the late 1990s. Inter-series correlations have been calculated between CRU and the raingauge based rainfall since they are based on gauge observations and are available for the same period 1929–1999. The results show positive and significant correlations (at the 5 percent level) for the whole of Amazonia and its northern and southern basins.

Given the possible regional discrepancies in rainfall variability, northern and southern Amazonia have been analysed separately. In northern Amazonia, the NAR index shows that rainfall exhibits a negative trend statistically significant at 5% level for the period 1948–99 (Fig. 2b), statistically significant at 5% from the Mann-Kendall test. NCEP rainfall and the CMAP datasets show a positive trend. In southern Amazonia, rainfall from gauge observation and from the gridded datasets CRU, CMAP and the NCEP rainfall show a positive trend also significant at 5% level. Long-term rainfall variability from our raingauge based estimates is similar to those derived from the CRU dataset. All rainfall indices show the reduced rainfall during the strong El Niño events during the 1980s and 1990s (Fig. 2c).

For the whole of Amazonia, Table 1 shows the size of the trends over given periods, since it is difficult to detect trends in Fig. 2. For the period 1929–99, the CRU and the raingauge-based indices in Amazonia exhibit negative but significant trends, while the CMAP shows a steep negative trend since the early 1980s, when it became available. The positive trends in the NCEP rainfall may be related more to assimilation of observational and satellite data since the middle 1970s. The GHCN shows the positive trends already discussed by Chen et al. (2001). At regional level, all indices show negative tendencies in northern Amazonia regardless of the period of the series, while in southern Amazonia the trends are positive in the CRU, raingauge-based dataset, while the CMAP dataset shows negative trends.

Perhaps the most remarkable feature in the rainfall variability in northern and southern Amazonia, is the presence of alternating periods of relatively wetter and drier periods. These periods are even more important than the unidirectional trends detected in Fig. 2a–c. Figure 3a and b shows the NAR and SAR indices normalized rainfall departure series for the whole 1929–1999 period. While they show opposite tendencies, both indices exhibit the negative rainfall departure during the intense El Niño events of 1982–84, 1986–87 and 1997–98. The NAR series exhibit relatively drier periods after the

Table 1. Linear trends in rainfall indices in the entire Amazonia, and the northern and southern basins. The star (*) shows significance at 5% level. Trends are represented in percentages of the mean, and in mm day^{-1} per decade. The periods of the time series are also shown

Index	Mean (mm day^{-1})	Period	Trend (mm day^{-1} dec^{-1})	Trend (%)
a) All Amazonia				
GCHN**	8.3	1957/99	+0.46*	+5.0*
NCEP	5.8	1950/99	+0.13	+11.0
CMAP	5.3	1980/99	−0.87	−20.0
CRU	5.5	1948/99	−0.16*	−12.0*
RAIN	5.9	1948/99	−0.15*	−17.0*
b) Northern Amazonia				
NCEP	6.5	1950/99	−0.15	−11.0
CMAP	6.1	1980/99	−0.52	−16.0
CRU	6.7	1948/99	−0.16*	−17.0*
RAIN	7.0	1948/99	−0.19*	−17.0*
c) Southern Amazonia				
NCEP	5.2	1950/99	+0.19	+18.0
CMAP	4.7	1980/99	−0.58	−23.0
CRU	5.1	1948/99	−0.08	−08.0
RAIN	4.3	1948/99	+0.08	+09.0

** Chen et al. (2003)

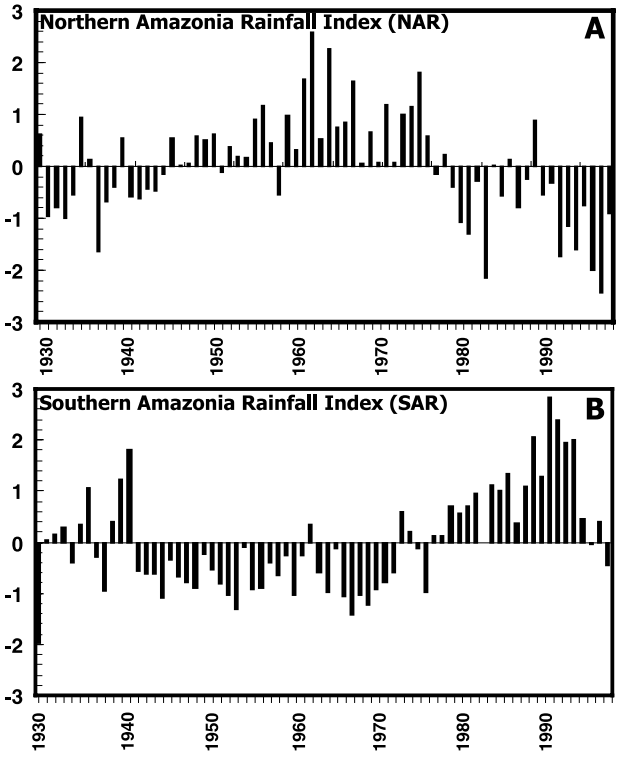

Fig. 3. Rainfall indices in northern (NAR) and southern Amazonia (SAR) from 1929/30 to 1998/99. Indices are expressed as departures normalized by the standard deviation, from the reference period 1949–1998

middle 1940s and 1970s, with a relatively wet period in between. This wetter period in the 1970s has also been reported in earlier publications based on observed rainfall and river data (Rocha et al., 1989; Gentry and Lopez Parodi, 1980), and at the time this was considered as an indicator of increased rainfall in the basin. This drier period after 1975 is consistent with the presence of stronger and more frequent El Niño events during 1983, 1987, 1991–93, and 1998 which tend to produce less rainfall in northern Amazonia. Southern Amazonia shows a period of relatively drier conditions from the early 1940s to the middle 1970s, and wetter conditions after that. In this case, transition periods are detected a bit earlier (1940–45) from wetter to drier conditions and during the middle 1970s. This is the opposite of the trends detected in northern Amazonia.

In order to explore whether rainfall changes during the periods 1929–45, 1946–75 and 1976–99 are statistically significant, a ''t-test'' was performed for the rainfall series in northern and southern Amazonia (Table 2). The analyses using the mean and standard deviations of rainfall in each period in both northern and southern Amazonia shows that in fact, the only significant difference is between 1946–75 and 1976–99 in

Table 2. Differences between 1929/25–1946/75 and 1946/75–1976–99 rainfall periods in northern and southern Amazonia. Mean and standard deviations (STD) are shown. Differences among periods are between the calculated values of ''t'' and the ''t'' values obtained from tables for each period and region

Period	Mean ($mm\ day^{-1}$)	STD ($mm\ day^{-1}$)	Differences	Statistical significance
a) Northern Amazonia				
1929/45	201.1	16.1	1929/46 versus 1946/75	No
1946/75	226.5	17.6	1946/75 versus 1976/99	No
1976/99	188.7	21.6		
b) Southern Amazonia				
1929–45	147.2	16.6	1929/46 versus 1946/75	No
1946–75	137.5	8.8	1946/75 versus 1976/99	Yes (99%)
1976–99	164.9	15.5		

southern Amazonia, where the increase of rainfall reaches statistical significance at the 99% level.

Figures 2 and 3 show that southern Amazonia exhibits excesses of rain during some El Niño events (1982–83, 1991–92, 1997–98) during the 1948–99 period. Ronchail et al. (2002) have suggested that these excesses occur also during austral wintertime, and so rainfall anomalies in southern Amazonia could be attributed to enhancement of the activity of extratropical perturbations during some El Niño years, and the ENSO related rainfall anomalies in this region are partly similar to those described in southeast South America (Liebmann et al., 1999; Seluchi and Marengo, 2000; Grimm et al., 1998, 2000). Furthermore, recent work by Obregon and Nobre (2003) have identified shifts in the rainfall regime in the mid-1970s for northwestern Amazonia and southern Brazil, with positive and significant trends since 1973 for southern Brazil, and with negative and significant trends since 1975 for northwestern Amazonia. Even though Obregon's analyses were performed using one representative station in each region and for the month with the peak rainfall, their results for northwestern Amazonia resemble those from northern Amazonia in Fig. 3a, with a shift in the rainfall regime in 1975. Furthermore, their conclusions for southern Brazil also seem to be applicable to southern Amazonia, since both regions show positive rainfall trends since 1973, as shown in Fig. 3b.

The observed rainfall shifts in the mid-1940s and 1970s on the rainfall regime in Amazonia detected by the NAR and SAR gauge-based indices (Fig. 3a, b) are also detected in the normalised time series rainfall indices based on the CRU dataset for the same regions as shown by Botta et al. (2002). The decadal scale variations detected in Fig. 3 may be better studies using spectral analyses. However, with a series of less than 70 years it is hard to identify decadal scale variations and these modes may appear only twice in the NAR and SAR series. The power spectra of the 1929–1998 NAR and SAR indices show several preferred time-scales of variability: NAR shows a mode of 13 and a short-term mode of 5 years, while SAR shows preferred time-scales of variability at 26, 17 and 8 years. Only the 26-year peak at SAR shows significance at 90% level.

To study these variations more carefully, we used the Singular Spectrum Analyses (SSA), a data-adaptive filter that is appropriate for short-term noisy series (Botta et al., 2002). SSA decomposes a time-series into its orthogonal basis functions; the eigenvectors with largest eigenvalues represent the greatest variability in the data. We performed SSA on the 1929–1998 NAR and SAR indices. For NAR, 15% of the variance is explained by the 13-year mode, while 11% of the variance is explained by the 5-year mode. SAR shows that the 26-year model explains 22% of the total variance while the 17-year mode explains 11% of the variance. From the analysis of Figs. 2 and 3, the short-term or interannual mode ($\sim$5 years) in northern Amazonia is associated with climate variability typical of the El Niño phenomenon, also shown in previous studies (Richey et al., 1999; Marengo, 1992; Marengo and Hastenrath, 1993; Uvo et al.,

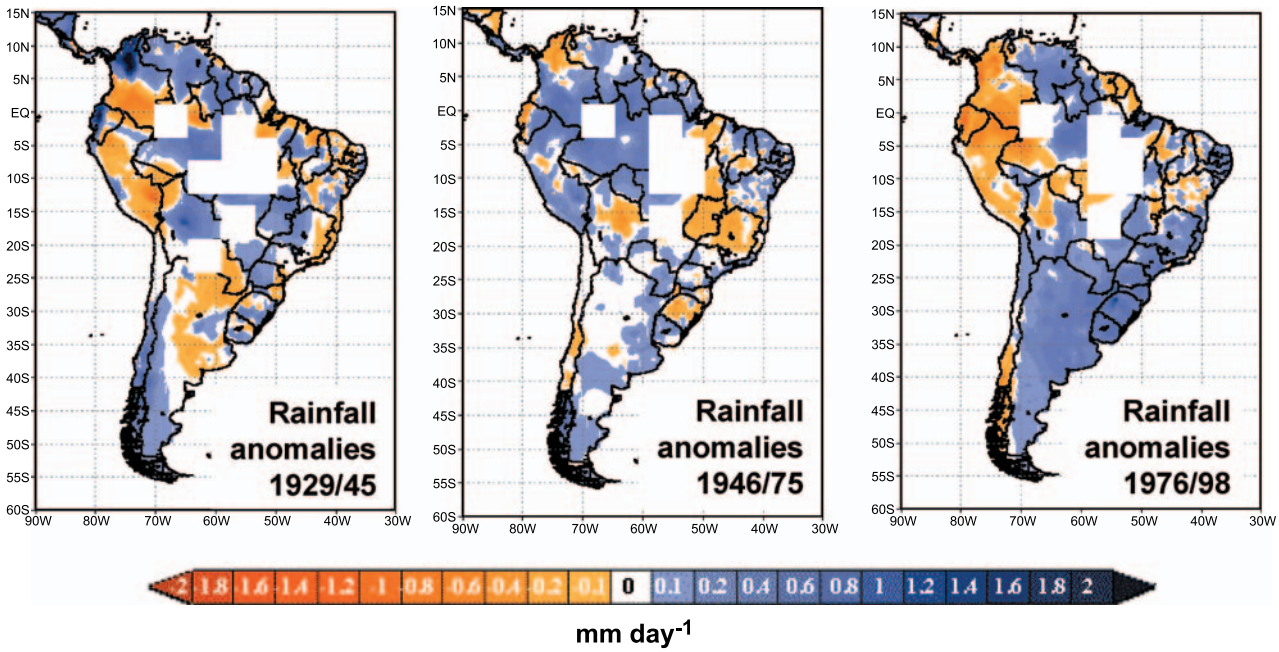

Fig. 4. Rainfall anomalies for decades in South America, as derived from the CRU rainfall data sets. (**a**) 1929/45, (**b**) 1946/75, (**c**) 1976/99. Anomalies are from the 1901–1999 long term mean. Colour scale is shown on the lower side of the panel

1998; Fu et al., 1999; Botta et al., 2001). The 13 and 26 year modes for a NAR and SAR respectively suggest decadal times scale variability. Botta et al. (2001) found a peak at 24–28 years in the entire Amazon Basin that explains 26% of the variance of precipitation, using the CRU dataset. It may be possible that this mode represents more the southern section of the basin as compared to the northern basin, showing the latter similar contribution from both the decadal and interannual mode.

Southern Amazonia is the region that exhibits the largest deforestation rates (http://www.inpe.br/amz.html) and if in fact we consider the reduced rainfall patterns derived from numerical models under regional deforestation, there is some conflict between the reduced rainfall we would expect due to increased deforestation and the positive rainfall trends observed in this part of the basin. In this regard, the effects of Amazonian deforestation on the regional hydrological cycle are still uncertain. Many modelling studies have predicted that large-scale conversion of the Amazonian rainforest into pasture, or croplands will tend to increase temperature and reduce both precipitation and evapotranspiration (Lean and Warrilow, 1989; Shukla et al., 1990; Nobre et al., 1991; Polcher and Laval, 1994a, b; Sud et al., 1996a, b; Lean and Rowntree, 1997; Hahmann and Dickinson, 1997; Costa and Foley, 2000). However, the rainfall trends in southern Amazonia do not show any significant reduction associated with increased deforestation or any changes in land-use in this sub-basin. Therefore, it seems that the climate shifts identified during the middle 1940s and the middle 1970s are of a climatic nature and not due to changes in land use in the basin.

3.2 The 1975–76-shift regime in the Pacific sector and its impacts on Amazonian rainfall

In this study, we are able to identify the shifts in rainfall regime in 1945–46 and in 1975–77 in the Amazon region. There is a prevalence of warm El Niño events in the post-1976 era (Trenberth, 1990; Trenberth and Hurrell, 1994; Zhang et al., 1997), with the past 25 years showing the two biggest El Niño events on record (1982–83 and 1997–98), and the longest on record in 1990–94. In addition, IPCC (2001) have identified a relatively wet period in Northeast Brazil during 1946–75 and drier periods from 1976–99, while

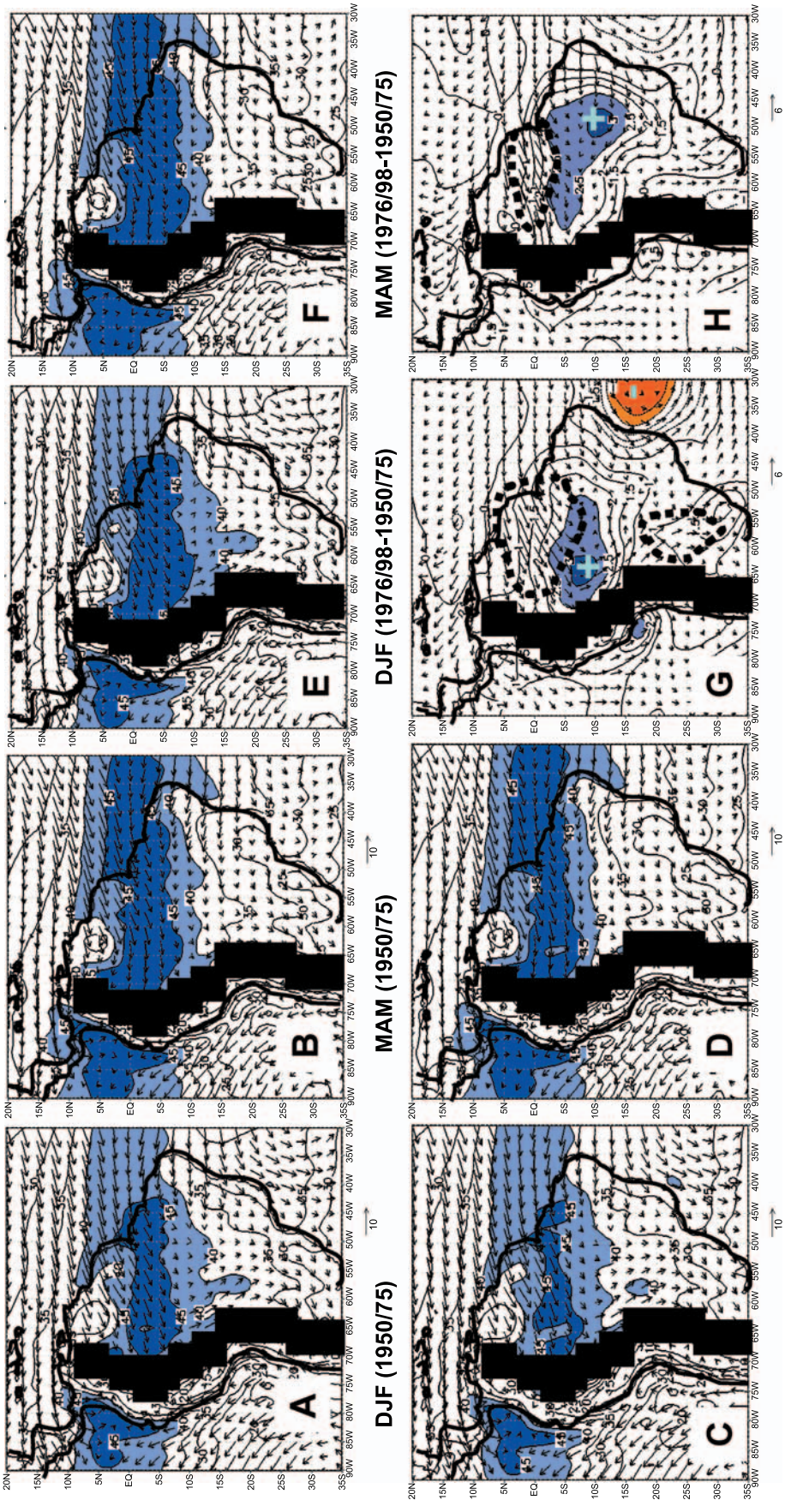

Fig. 5. DJF and MAM seasonal means of 850 hPa winds ($m\,s^{-1}$) and vertically integrated precipitable water ($g\,kg^{-1}$) from NCEP reanalyses. (**A**) DJF 1950/98, (**B**) MAM (1950/98), (**C**) DJF (1950/75), (**D**) MAM (1950/75), (**E**) DJF (1976/98), (**F**) MAM (1976/98), (**G**) Difference 1976/98–1959/75, (**H**) Difference 1976/98–1959/75. Wind scale is shown at the lower right side of each panel. Statistical significance at 5% is shown inside the broken lines

the tendencies in the Amazon basin are not clear due to the lack of complete data coverage in the basin. The climate shift in 1975 has been identified and studied in previous papers linking this variability to El Niño-like conditions as represented by the 1975–99 positive Pacific Decadal Oscillation PDO phase (Zhang et al., 1997). The phases of the PDO have been linked to anomalously warm and cold surface conditions in several parts of the world and to changes in the volumes of salmon catch on the Northwest coast of the US (Mantua et al., 1997). Villalba et al. (1997) analyze trends using tree-ring records at high elevations in northern Patagonia, and they also found an abrupt rise in temperature commencing in 1977, consistent with North Pacific basin warm climatic conditions while cool conditions prevailed in the Central North Pacific, consistent with the variations in the PDO. Their reconstructions show that long-term intervals of above average temperature have been previously recorded in the recent past.

Since 1976, such anomalies in Pacific Ocean temperatures and in weather extreme events have become more frequent, more intense, and longer lasting than in the preceding 100 years, as indicated in records kept since 1877. Widespread agreement that a climate shift, with extensive ecosystem impacts, occurred in the central Pacific during 1976/77. The 1975–77-regime shift appears to follow earlier shifts in 1925 and 1947 (IPCC, 2001). The climate shift in the mid-1970s appears to have modified the amplitude of the annual rainfall cycle and its spatial distribution, as suggested by Obregon and Nobre (2003). Figure 4a–c shows rainfall anomalies during the periods 1929–45, 1946–75 and 1976–98, as derived from the CRU dataset, using as reference the 1961–90 period, considering the climate shifts from the mid-1940s and the mid-1970s. The whole of Amazonia and northern Northeast Brazil showed above normal rainfall during 1946–75; while during 1976–98 only the eastern section of the basin showed rainfall above normal, while the rest of the Amazon region exhibited negative rainfall anomalies. Figure 4c also shows the positive rainfall anomalies in southern Brazil and northern Argentina, as suggested by previous studies (Barros et al., 1999; Obregon and Nobre, 2003).

3.3 Large-scale circulation change in the 1975–76 period and rainfall variations in Amazonia

Dettinger et al. (2000b), IPCC (2001) and several references quoted therein have identified three periods with changes in rainfall regime around the world: the mid-1910s, 1940s and 1970s. However, they did not mention any impact on the behaviour of rainfall in the Amazon basin during those periods. The current study shows weak positive trends of basin-wide rainfall across Amazonia, with shifts in the rainfall regime on decadal time scales in the mid-1940s and 1970s, and with contrasting tendencies in the northern and southern sections of the basin.

Although a periodicity of 25–30 years of relatively wetter and drier conditions in northern and southern Amazonia may be apparent in Fig. 3, such a cycle cannot be put forward on the basis of this relatively short run of data, because the series are not much longer than this cycle. Visual inspection of Fig. 3 also does not entirely support this contention. Chen et al. (2001, 2003) identified an increase in rainfall in the period 1978–98 as compared to the period (1958–77), and they linked this tendency to interdecadal variations in the global divergent circulation before and after 1977, with the circulation features derived from the NCEP reanalyses. Their analysis suggests an intensification of the near-surface branch of the Walker cell, exhibiting an increase in low-level moisture convergence over the entire basin, and thus increasing rainfall trends in the basin during the period 1978–98 as compared to 1959–77. The fact that Chen and collaborators used more raingauge stations south of 5° S (equivalent to our SAR region) may suggest that the increasing trends they found may be applicable to southern Amazonia only. Trying to be consistent with the analyses by Chen et al. (2001) before and after 1977, the maps of Fig. 5a, b show the NCEP-derived low level circulation and integrated precipitable water in tropical South America during December–January–February (DJF) and March–April–May (MAM), which are the rainiest months in southern and northern Amazonia, respectively, for the periods 1950–75 and 1976–98. The wind and precipitable water climatologies show the intense northeast trades over the tropical North Atlantic flowing into the

Amazon basin and then the deflection of the winds towards southern Brazil due to the Andes during DJF. In MAM, also observed are the intensified northeast trades and the large amount of precipitable water over central Amazonia and northern Northeast Brazil, consistent with the peak of the rainy seasons over those regions.

Similar features are found in the climatology for the 1950–75 and 1976–98 individual periods (Fig. 5c–f). However, the difference maps (Fig. 5g, h) show two main features: (a) the intensification of the Northeast trades from the tropical North Atlantic into the Amazon basin during both DJF and MAM in 1976–98 as compared to 1950–75, and (b) the relative humidification of the central Amazon basin associated with the increased moisture transport from the tropical North Atlantic into Amazonia and the increased precipitable water in central Amazonia.

This tendency is consistent with the positive trends in the NCEP derived moisture convergence into the Amazon basin-tropical Atlantic sector and rainfall over those regions, as suggested by various studies using the reanalyses (Chen et al., 2001, 2003; Curtis and Hastenrath, 1999; Hastenrath, 2001), and the positive trends in all-Amazon rainfall from the NCEP reanalyses as shown in Fig. 2a. This increased moisture

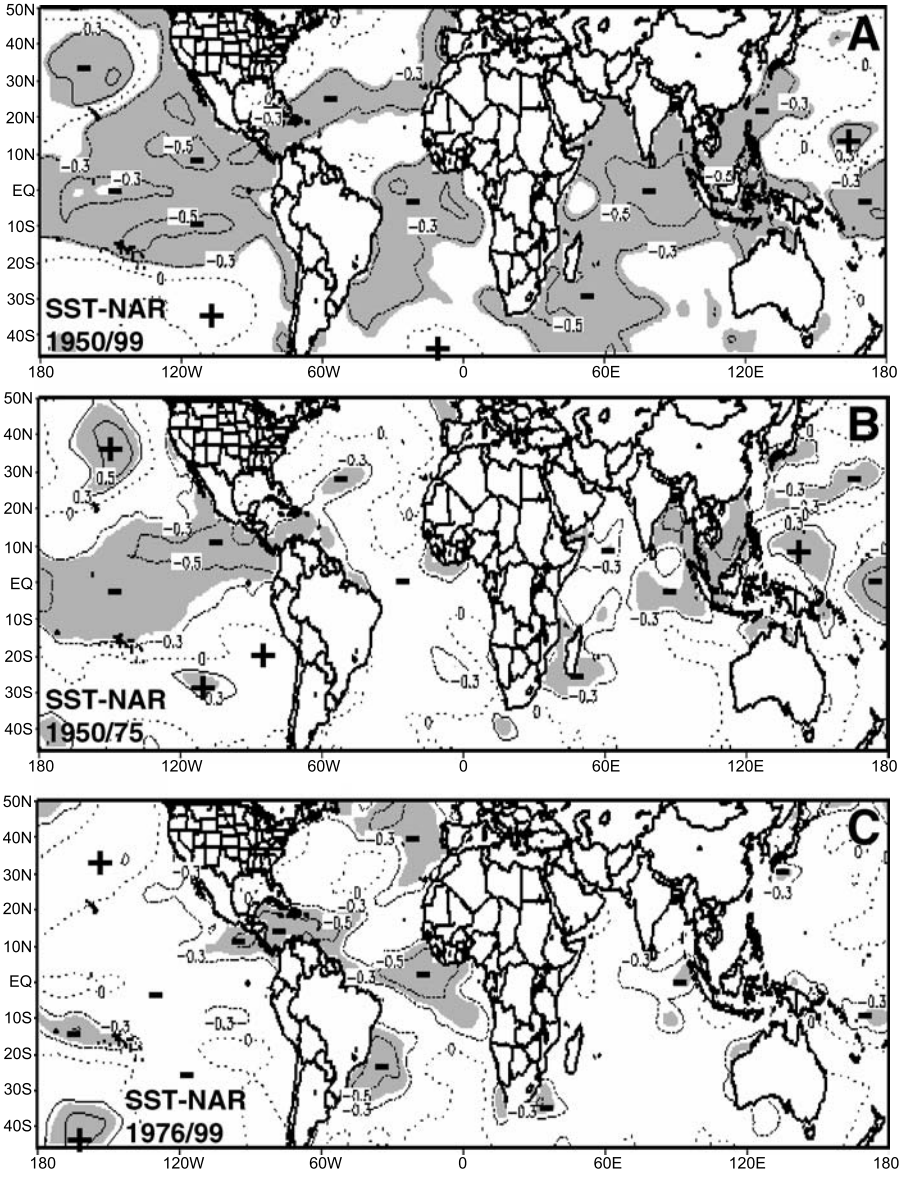

Fig. 6. Correlation coefficients between tropical SSTs (November) and NAR and SSTs (January) and SAR. (**A**) SST-NAR 1950/99, (**B**) SST-NAR (1950/75), (**C**) SST-NAR (1976/99), (**D**) SST-SAR (1950/99), (**E**) SST-SAR (1950/ 75), (**F**) SST-SAR (1976/ 99). Contours are plotted for the zero line (broken), and the ±0.3 and ±0.5 values. Signs "+" and "−" in the maps indicate the sign of the correlation coefficients. Statistical significance at 5% is shown in grey shaded areas

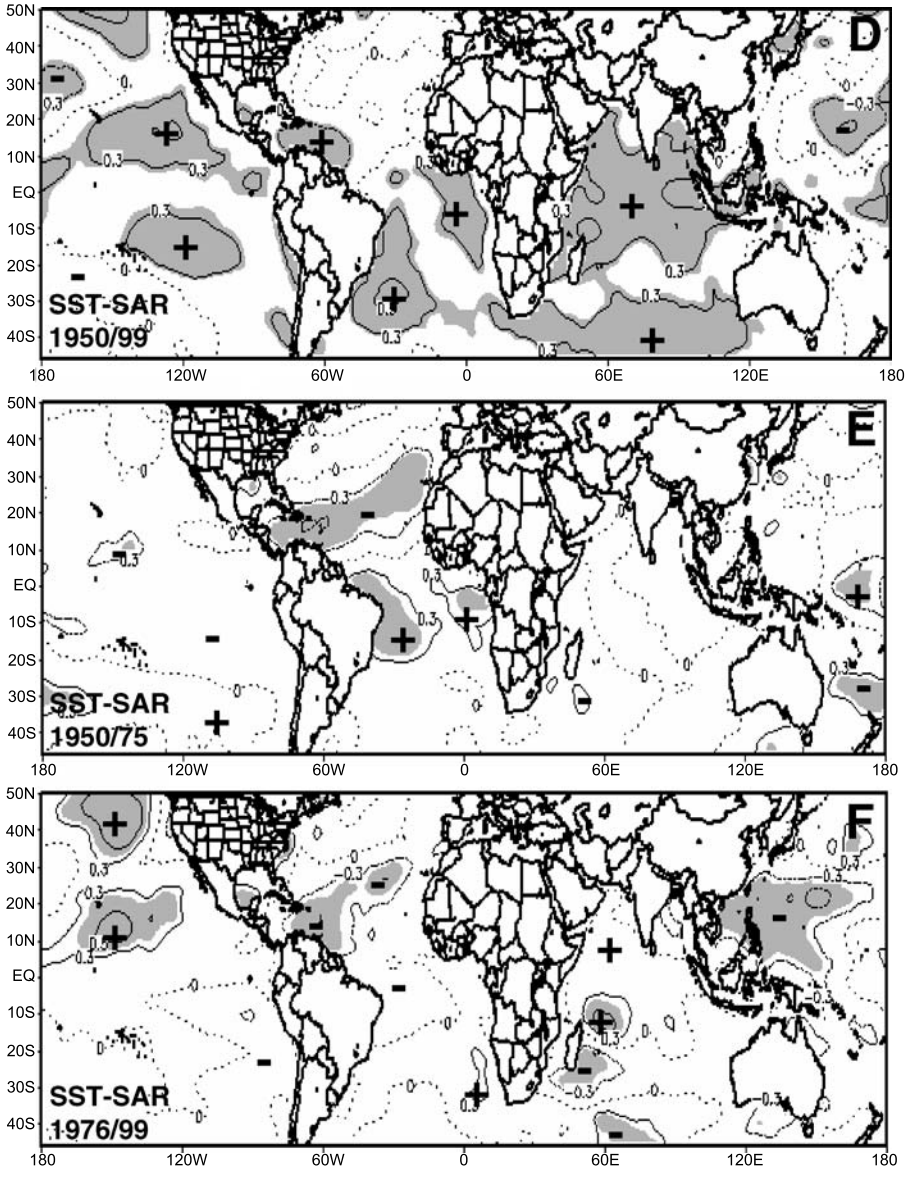

Fig. 6 (*continued*)

transport from the tropical Atlantic into tropical South America has been detected in previous studies by Wagner (1996) and Hastenrath (2001), and to the observed positive trends observed in Northeast Brazil since 1900 as reported in the IPCC (2001) report, and in earlier publications (Hastenrath and Greischar, 1993; Wagner, 1996; Marengo et al., 1998).

Therefore, the circulation and moisture transport field changes in the mid-1970s, derived from the NCEP reanalyses, suggesting a tendency for increased moisture transport and possibly rainfall over the whole of Amazonia after 1975/76. However, when considering the regional rainfall indices trends in Figs. 2 and 3, it seems that this humidification of the basin derived from the analyses of circulation and moisture might be linked to the positive trends in southern Amazonia, while still not explaining the observed slightly negative rainfall trends in northern Amazonia.

However, conclusions from Fig. 5 and from Chen et al. (2001, 2003) could be affected not only by shifts in circulation regimes, but also by changes in the way the NCEP reanalyses were produced. With the inclusion of satellite data in the late 1970s the reanalyses generally improved for most regions of the globe. Prior to that time, the analyses depend greatly on available radiosonde data. Given the sparse observational net-

work over South America, most circulation features are model dependent. The GCM that was used in the reanalysis was a version of NCEP's operational medium range forecast model, with a rather coarse resolution (approximately $2.5° \times 2.5°$ lat-long). So much of the information on wind and moisture climatology for the region based on the NCEP reanalyses reflects the model climatology. According to Kousky (personal communication), a couple of problems occurred in the reanalysis that affect the reliability of analyses over South America on various time scales. The diurnal cycle was poorly treated and there are many inconsistencies in the related radiation, cloud, precipitation, divergence and vertical motion.

3.4 SST and near surface circulation changes linked to decadal scale rainfall variability in Amazonia

Interdecadal changes in both northern and southern Amazonian rainfall are studied in the context of changes in oceanic and atmospheric conditions in the tropical oceans. We calculate correlation fields between SST, U and V during January/November and the NAR/SAR rainfall indices, respectively for the period 1958–98 and for the sub-periods 1950–75 and 1976–99.

The SST correlation map (Fig. 6a) shows that during the 1950–99 period, deficient rainy seasons in northern Amazonia are related to anomalously warm surface waters in the tropical

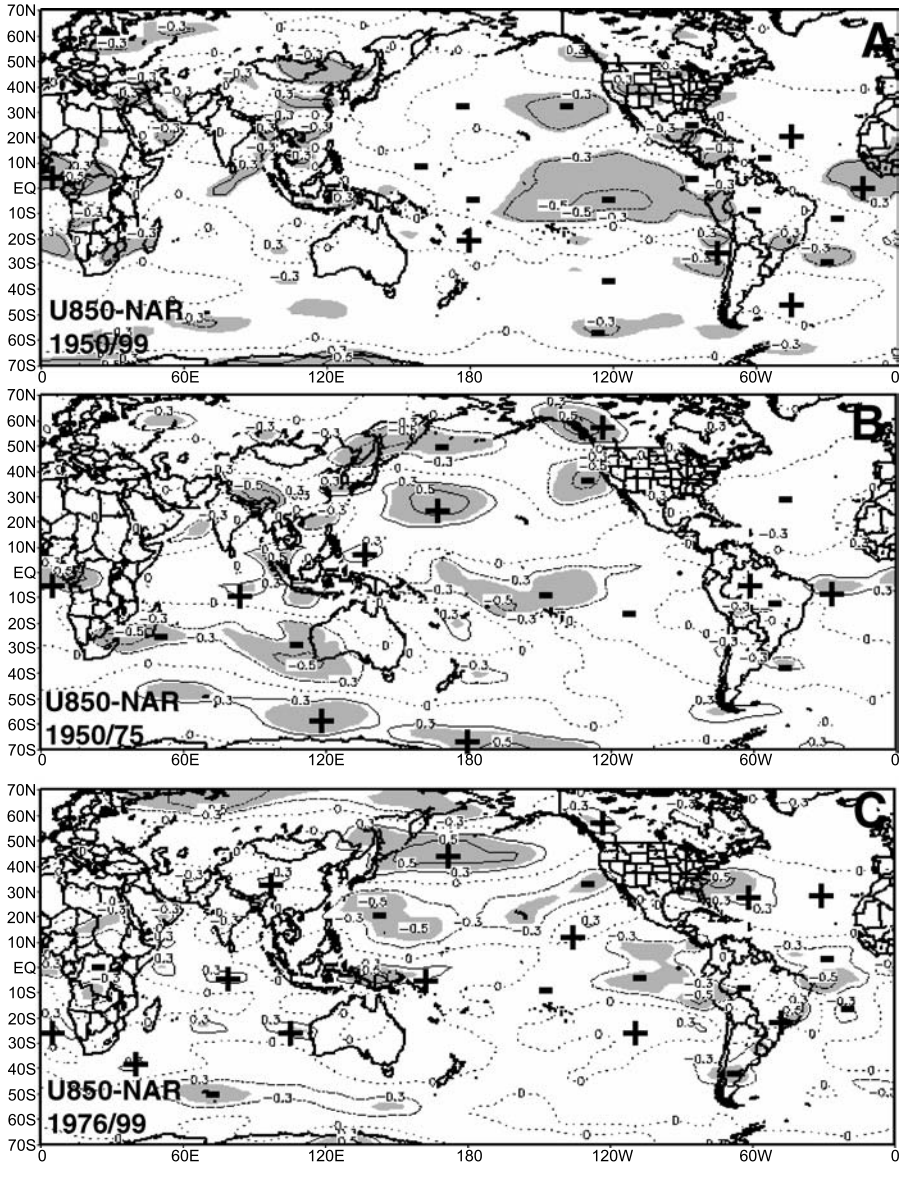

Fig. 7. Correlation coefficients between U and V components of the wind at 850 hPa and rainfall in Northern Amazonia. (**A**) U850-NAR (1950/99), (**B**) U850-NAR (1950/75), (**C**) U850-NAR (1976/99), (**D**) V850-NAR (1950/99), (**E**) V850-NAR (1950/75), (**F**) V850-NAR (1976/99). Correlation coefficient values appear on the colour bar on the lower side of each panel. Contours are plotted for the zero line (broken), and the ± 0.3 and ± 0.5 values. Signs "+" and "−" in the maps indicate the sign of the correlation coefficients. Statistical significance at 5% is shown in grey shaded areas

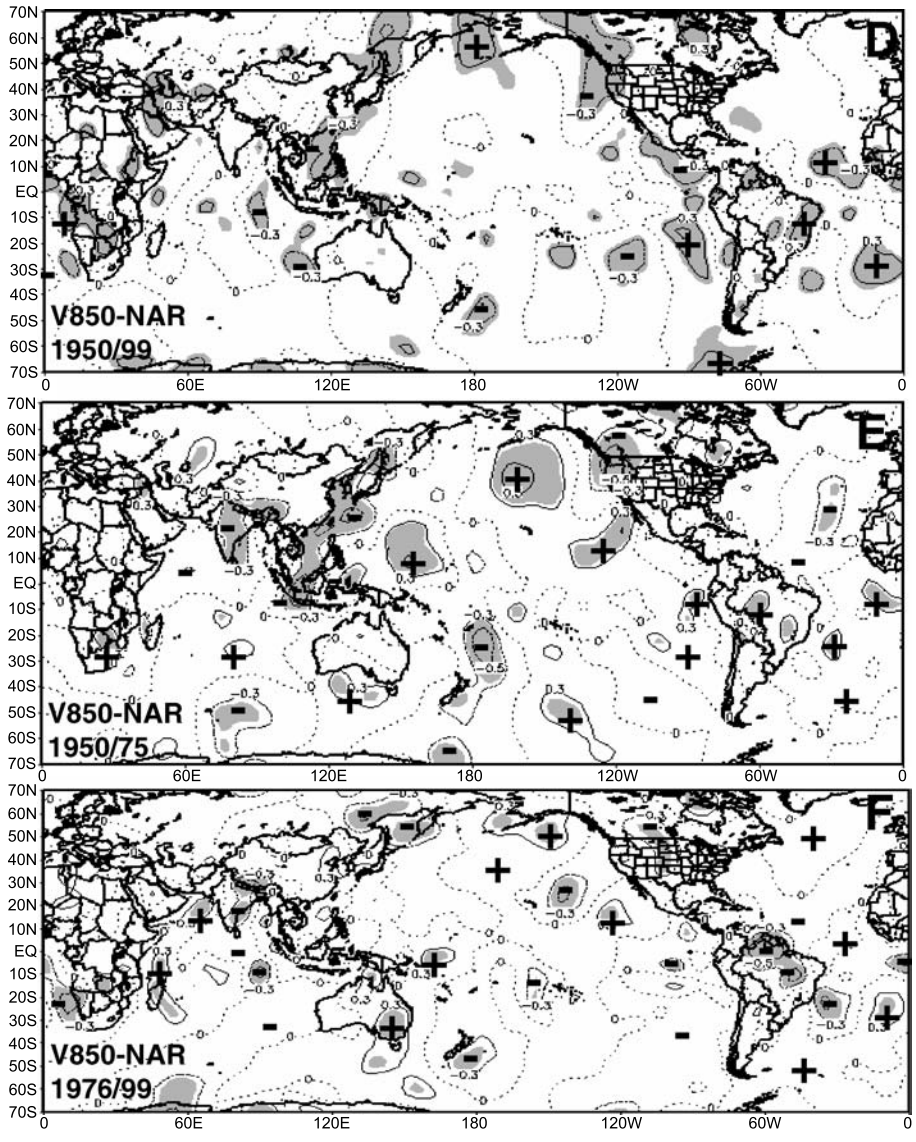

Fig. 7 (*continued*)

central and eastern Pacific Ocean, the tropical North Atlantic, the South Atlantic and Indian Oceans during January, reaching field significant at 5% over those regions. In southern Amazonia, Fig. 6d shows that abundant rainy seasons in southern Amazonia are consistent with anomalously warm surface waters in the tropical south Pacific, and East Atlantic and the Indian Ocean in November, showing a contrasting pattern with the SST correlations for rainfall anomalies in northern Amazonia.

During the 1950–75 period (Fig. 6b) the relatively deficient rainy seasons identified for northern Amazonia during this period were characterized by anomalously warm surface waters in the tropical Atlantic north of the equator and in the central and eastern Pacific, while during 1976–99 (Fig. 6c) the deficient rainfall in northern Amazonia is associated with anomalously warm surface waters in the tropical north Atlantic and to a lesser degree with warm surface in the tropical Pacific. These SST patterns are consistent with the deficient rainy seasons during the El Niño in 1983, 1987 and 1998 where warm surface water dominates most of the tropical and equatorial Atlantic and the tropical North Atlantic. For southern Amazonia (Fig. 6d–f) the correlation fields indicate that abundant rainy seasons in southern Amazonia are consistent with warm surface water in the central Pacific and on the tropical Atlantic between 0° and 20° S during 1950–99, while during the 1950–75 and 1976–99 the correlations are low for the tropical Pacific, the anomalously wet period of

1950–75 is consistent with the positive correlations in the tropical Atlantic south of the equator.

The circulation fields (Fig. 7a, f) show that during the 1950–98 period, deficient rainy seasons in northern Amazonia are characterized by weakened northeast trades over the tropical Atlantic and anomalous flow from the west along the equatorial Pacific. For southern Amazonia (not shown), deficient rainy seasons in northern Amazonia were associated with weakened Atlantic northeast trades over the region. During 1950–75 (Fig. 7b, e), abundant rainy seasons in northern Amazonia show larger negative correlation with the U and V fields in the tropical North Atlantic suggesting enhanced northeast trades into the basin. However the correlations in the tropical Pacific are not so revealing. On the other hand during 1976–99 (Fig.7c, f), the U and V correlation fields suggest a stronger impact of the tropical Pacific, with stronger westerlies over the equatorial Pacific and reduced northeast flow typical of weak rainy seasons in northern Amazonia. The fact that these patterns resemble El Niño mode, imply the presence of more frequent and intense El Niño events in 1976–98 (with an active role of the tropical Pacific), while during 1950–75 the tropical Pacific was less active. Correlation fields between rainfall in southern Amazonia and SST (Fig. 6d–f) and circulation fields (not shown) do not show a revealing pattern of circulation linked to El Niño signal in the Pacific as they do in the northern Amazonia, while the tropical Atlantic shows similar circulation features linked to abundant or deficient rainy seasons in southern Amazonia similar to those of northern Amazonia.

4. Conclusions

To obtain accurate estimates of precipitation rates across the Amazon basin is a significant challenge, because it has few raingauge stations in a region that is one of the rainiest on the planet. The different estimates provide a general pattern that may have a consistent tendency, but with differences among datasets reaching up to 4 to 6 mm day^{-1}.

In relation to tendencies, our study suggests that for the entire Amazon basin, rainfall exhibits downward trends based on the CRU, CMAP, and our raingauge-based indices. However, the GHCN and the NCEP rainfall analyses show positive trends. In fact, the upward trends from the NCEP rainfall are supported by circulation changes that favour an increase of moisture transport into Amazonia. When we ''break'' the Amazon region into the southern and northern sub-basins, the negative trend is maintained for northern Amazonia, while southern Amazonia exhibits a slight positive trend, as shown by our raingauge-based NAR and SAR rainfall indices, and confirmed by the CRU rainfall. However, more important than these trends are the decadal scale changes in both sections of the basin, and with a shift in the rainfall on both sides of the basin during the middle 1940s and 1970s.

For northern Amazonia, the weak negative rainfall trends are not consistent with the increased moisture transport, suggesting that moisture convergence flux may not be an effective means to maintain Amazonian rainfall. However, the fact that there are very few upper-air stations in Amazonia, especially in the north and centre (the wettest regions of Amazonia) to report data to be assimilated into the NCEP model that produced the reanalyses, introduced some degree of uncertainty in the moisture derived fields in this part of the basin.

The decadal analysis suggests shifts in Amazonian rainfall regime in the mid-1940s and the mid-1970s, where northern Amazonia had relatively wetter conditions during the 1945 to 1975, and relatively drier conditions between 1975 and 1998. This latter period was characterised by a more active tropical Pacific, with more frequent and stronger El Niño years, as compared to before 1975 where strong El Niño events were less frequent.

For the period between the mid-1940s and the mid-1970s, rainfall in northern Amazonia was above normal, while after 1976 rainfall tended to be below normal. These tendencies, detected with raingauge-based indices, are supported by increases in the NCEP derived circulation and moisture transport into Amazonia during the 1946 to 1976 period, as compared to 1976 to 1999. The negative trends detected for the entire Amazon Basin seems to be more relevant to the northern section of the basin, as compared to the southern basin. The southern section of the Amazon basin seems to show similarities with observed rainfall changes in southern Brazil and northern Argentina, where positive rainfall

trends have been detected since the early 1970s. These trends are linked to increased activity of extra-tropical perturbations that are typical of El Niño years, and have been more frequent since 1975. Thus, rainfall in the Amazon basin is impacted by El Niño: in the northern part linked to austral summertime anomalies in the zonal and meridional circulations with abnormal subsidence in the region, and rainfall anomalies in the southern part of the basin are linked to springtime extra tropical circulation anomalies (such as midlatitude extra tropical perturbations) that normally affect southeast South America at this time of the year. The proven associations between SST anomalies in the tropical Pacific and rainfall anomalies in northern Amazonia corroborate the fact that in the decades with more intense and frequent El Niño events, between 1976 and 1998, relatively less rainfall was detected in northern Amazonia, as compared to the period 1950–75. This is also supported by the changes in the near surface circulation along the tropical Pacific and Atlantic, where the correlation fields between 1976 and 1999 contain features of circulations typical of strong El Niño years and drier conditions in northern Amazonia. This tendency is not so obvious in southern Amazonia, where decadal changes in rainfall anomalies associated with changes in SST in the tropical Pacific are not clearly identified. The positive correlations in the tropical south Atlantic show a pattern of warmer surface water and increased rainfall in southern Amazonia before 1975. Thus, particular regions of the basin have their own response to El Niño at interannual scales, and at interdecadal scales there is a teleconnection between the north Pacific climate shift and the long-term rainfall variability all across the Amazon basin.

In summary, these results provide observational evidence that depicts a complex picture of long-term climate variability in the Amazon basin, in which the Pacific and Atlantic oceans, and rainfall across the Amazon basin vary at interannual and decadal time scales. Variability in the SSTs of the tropical Pacific and Atlantic is likely to play an important role in driving the interdecadal variability in Amazonia's rainfall.

In the context of the Global Energy and Water Balance Energy programme, GEWEX, work is in progress to investigate the long-term variations in the water balance components of the Amazon basin and its possible connections with changes in land use in the region, as well as to changes in large scale circulation associated with changes in moisture transport into and out off the Amazon basin. In addition, we are also implementing comparisons between observed and reanalyses precipitation datasets, on interannual, decadal and long-term modes of variability for other regions of the world.

Acknowledgements

The NCEP/NCAR reanalyses were provided by NCAR. I would like to thank ANEEL and CPTEC for providing rainfall station data. JM was partially funded by the Brazilian National Science and Technology Council (CNPq).

References

Barros V, Castañeda ME, Doyle M (1999) Recent precipitation trends in South America to the East of the Andes: an indication of climatic variability. In: Volheimer W, Smolka P (eds) Southern Hemisphere Paleo and Neoclimates: Concepts and problems. Berlin, Heidelberg: Springer

Botta A, Ramankuttym N, Foley JA (2002) Long-term variations of climate and carbon fluxes over the Amazon Basin. Geophys Res Lett 29: 564–579

Chen TC, Yoon JH, St. Croix K, Takle E (2001) Suppressing impacts of the Amazonian deforestation by the global circulation change. Bull Amer Meteor Soc 82: 2210–2216

Chen TC, Takle ES, Yoon JH, St. Croix KJ, Hsieh P (2003) Impacts on tropical South America Rainfall due to changes in global circulation. In: Proceedings of the 7th International Conference on Southern Hemisphere Meteorology and Oceanography. Wellington, New Zealand, Ed. by American Meteorological Society, Boston, Massachusetts, pp 92–93

Chu PS, Yu ZP, Hastenrath S (1994) Detecting climate change concurrent with deforestation in the Amazon Basin: Which way has it gone? Bull Amer Meteor Soc 75: 579–583

Costa MH, Foley JA (1998) A comparison of precipitation data sets for the Amazon basin. Geophys Res Lett 25: 155–158

Costa MH, Foley JA (1999) Trends in the hydrologic cycle of the Amazon basin. J Geophys Res 104: 14189–14198

Curtis S, Hastenrath S (1999) Trend of upper-air circulation and water vapor over equatorial South America and adjacent oceans. Int J Climatol 19: 863–876

Dettinger M, Battisti D, McCabe G, Bitz C, Garreaud R (2000a) Interhemispheric effects of interannual and decadal ENSO-like variations of the Americas. In: Markgraf V (ed) Present and past interhemispheric climate linkages in the Americas and their societal effects. San Diego, London, Sydney, Tokyo: Academic Press, pp 1–14

Dettinger M, Cayan D, McCabe G, Marengo JA (2000b) Multiscale ENSO variability and hydrological systems. In: Diaz H, Markgraf V (eds) El Niño: Multiscale variability and its impacts on natural ecosystems and society. Cambridge University Press, pp 113–148

Dias de Paiva EMC, Clarke R (1995) Time trends in rainfall records in Amazonia. Bull Amer Meteor Soc 75: 579–583

Foley JA, Botta A, Coe MT, Costa MH (2002) The El Niño/Southern Oscillation and the climate, ecosystems and rivers in Amazonia. Global Biogeochemical Cycles (in press)

Fu R, Zhu B, Dickinson RE (1999) How do atmosphere and land surface influence seasonal changes of convection in the tropical Amazon? J Climate 12: 1306–1321

Fu R, Dickinson RE, Chen MX, Wang H (2001) How do tropical sea surface temperatures influence the seasonal distribution of precipitation in the equatorial Amazonia? J Climate 14: 4003–4026

Gentry A, Lopez-Parodi J (1980) Deforestation and increased flooding in the upper-Amazon. Science 210: 1354–1356

Grimm AM, Ferraz SET, Gomez J (1998) Precipitation anomalies in southern Brazil associated with El Niño and La Niña events. J Climate 11: 2863–2880

Grimm AM, Barros V, Doyle M (2000) Climate variability in Southern South America Associated to El Niño and La Niña events. J Climate 13: 25–58

Hahmann A, Dickinson R (1997) RCCM2 BATS model over tropical South America: application to tropical deforestation. J Climate 10: 1944–1964

Hastenrath S (2001) Interannual and longer-term variability of upper air circulation in the Northeast Brazil-Tropical Atlantic sector. J Geophys Res 105: 7327–7335

IPCC (2001) Climate Change 2001: The Scientific Basis. Contribution of Working Group I to the Third Assessment Report of the Intergovernmental Panel on Climate Change (IPCC). Cambridge University Press, Cambridge, UK, 944 pp

Kalnay E, Kanamitsu M, Kistler R, Collins W, Deaven D, Gandin L, Iredell M, Saha S, White G, Woollen J, Zhu Y, Chelliah M, Ebisuzaki W, Higgins W, Janowiak J, Mo K, Ropelewski C, Wang J, Leetma A, Reynolds R, Jenne R, Joseph D (1996) The NCEP/NCAR 40-Year Reanalyses Project. Bull Amer Meteor Soc 77: 437–471

Lean J, Rowntree P (1997) Understanding the sensitivity of a GCM simulation of Amazonian deforestation to specification of vegetation and soil characteristics. J Climate 6: 1216–1235

Lean J, Warrilow D (1989) Climatic impact of Amazon deforestation. Nature 342: 311–313

Liebmann B, Kiladis G, Marengo JA, Ambrizzi T, Glick J (1999) Submonthly convective variability over South America and the South Atlantic Convergence Zone. J Climate 12: 1877–1891

Liebmann B, Marengo JA (2001) Interannual variability of the rainy season and rainfall in the Brazilian Amazonia. J Climate 14: 4308–4318

Mantua J, Hare S, Zhang Y, Wallace JM, Francis R (1997) A Pacific interdecadal climate oscillation with impacts on salmon production. Bull Amer Meteor Soc 78: 1069–1080

Marengo JA (1992) Interannual variability of surface climate in the Amazon basin. Int J Climatol 12: 853–863

Marengo JA, Miller JL, Russell G, Rosenzweig C, Abramopoulos F (1994) Calculations of river-runoff in the GISS GCM: impacts of a new-land surface parameterization and runoff routing model on the hydrology of the Amazon basin. Clim Dynam 10: 349–361

Marengo JA, Nobre CA (2001) The Hydroclimatological framework in Amazonia. In: Richey J, McClaine M, Victoria R (eds) Biogeochemistry of Amazonia. Oxford, UK: Oxford University Press, pp 17–42

Marengo JA, Tomasella J, Uvo CRB (1998) Long-term streamflow and rainfall fluctuations in tropical South America: Amazonia, Eastern Brazil and Northwest Peru. J Geophys Res 103: 1775–1783

Marengo JA, Cavalcanti IFA, Satyamurty P, Nobre CA, Bonatti JP, Manzi A, Trosnikov I, Sampaio G, Camargo H, Sanches MB, Cunningham CAC, D'Almeida C, Pezzi LP (2002) Ensemble simulation of regional rainfall features in the CPTEC/COLA atmospheric GCM. Skill and predictability assessment and applications to climate predictions. Clim Dynam (in press)

Matsuyama H (1992) The water budget in the Amazon River basin during the FGGE period. J Meteorol Soc Jap 70: 1071–1083

New M, Hulme M, Jones P (2000) Representing twentieth-century space-time climate variability. Part II: Development of 1901–96 monthly grids of terrestrial surface climate. J Climate 13: 2217–2238

Nobre CA, Sellers P, Shukla J (1991) Amazonian deforestation and regional climate change. J Climate 4: 957–988

Nobre P, Shukla J (1996) Variations of sea surface temperature, wind stress, and rainfall over the tropical Atlantic and South America. J Climate 9: 2464–2479

NRC (1998) Decade-to-century-scale climate variability and change. A science strategy. Washington, D.C.: National Academic Press, 141 pp

Obregon G, Nobre CA (2003) A climate shift in mid-1970's in Northwest Amazonia and Southern Brazil. In: Proceedings of the 7th International Conference on Southern Hemisphere Meteorology and Oceanography. Wellington, New Zealand, Ed. by American Meteorological Society. Boston, Massachusetts, pp 88–89

Polcher J, Laval K (1994a) The impact of African and Amazonian deforestation on tropical climate. J Hydrol 155: 389–405

Polcher J, Laval K (1994b) A statistical study of the regional impact of deforestation on climate in the LMD GCM. Clim Dynam 10: 205–219

Rao VB, Chapa S, Franchito SH (1996) Annual variation of rainfall over Brazil and water vapor characteristics over South America. J Geophys Res 101: 26539–26551

Reynolds R, Smith T (1994) Improved global seas surface temperature analyses using optimum interpolation. J Climate 7: 929–948

Richey J, Nobre CA, Deser C (1989) Amazon River discharge and climate variability: 1903 to 1985. Science 246: 101–103

Ronchail J, Cochonneau G, Molinier M, Guyot JL, Chaves AGM, Guimaraes V, Oliveira E (2001) Interannual rainfall variability in the Amazon basin and sea-surface temperatures in the equatorial Pacific and the tropical Atlantic Oceans. Int J Climatol 22: 1663–1686

Robertson A, Mechoso CR (1998) Interannual and decadal cycles in river flows of Southeastern South America. J Climate 11: 2570–2581

Rocha H, Nobre CA, Barros M (1989) Variabilidade natural de longo plazo no ciclo hidrologico da Amazonia. Climanalise 4: 36–42

Russell G, Miller J (1990) Global river runoff calculated from a global atmospheric general circulation model. J Hydrol 117: 241–254

Seluchi ME, Marengo JA (2000) Tropical-Midlatitude exchange of air masses during summer and winter in South America: Climatic aspects and examples of intense events. Int J Climatol 20: 1167–1190

Shukla J, Nobre CA, Sellers P (1990) Amazonia deforestation and climate change. Science 247: 1322–1325

Stern W, Miyakoda K (1995) Feasibility of seasonal forecasts inferred from multiple GCM simulations. J Climate 8: 1071–1085

Sud Y, Yang R, Walke G (1996a) Impact of in situ deforestation in Amazonia on the regional climate: General circulation model simulation study. J Geophys Res 101: 7095–7109

Sud Y, Walker G, Kim JH, Liston GP, Sellers P, Lau W (1996b) Biogeophysical consequences of a tropical deforestation scenario: a GCM simulation study. J Climate 9: 3226–3247

Trenberth K (1990) Recent observed interdecadal climatic changes in the Northern Hemisphere. Bull Amer Meteor Soc 71: 988–993

Trenberth K, Hurrel J (1994) Decadal atmosphere-ocean variations in southern South America. Clim Dynam 9: 303–319

Uvo CRB, Repelli CA, Zebiak S, Kushnir Y (1998) The relationship between tropical Pacific and Atlantic SST and Northeast Brazil monthly precipitation. J Climate 11: 551–562

Villalba R, Boninsegna JA, Veblen TT, Schmelter A, Rubulis S (1997) Recent trends in tree-rings records from high elevation sites in the Andes of Northern Patagonia. Climatic Change 36: 425–454

Vose RS, Schmoyer RL, Steurer PM, Peterson TC, Heim R, Karl T, Eischeid JK (1992) The Global Historical Climatology Network: Long-term monthly temperature, precipitation, sea level pressure, and station pressure data. NDP-041. Carbon Dioxide Information Analysis Center, Oak Ridge National Laboratory, Oak Ridge, Tennessee

Wagner R (1996) Decadal-scale trends in mechanisms controlling meridional sea surface temperature gradients in the tropical Atlantic. J Geophys Res 101: 16683–16694

Xie P, Arkin P (1997) Global precipitation: a 17-yr monthly analysis based on gauged observations, satellite estimates and numerical model outputs. Bull Amer Meteor Soc 78: 2539–2558

Xie P, Arkin P (1998) Global monthly precipitation estimates from satellite-observed outgoing longwave radiation. J Climate 11: 137–164

Zeng N (1999) Seasonal cycle and interannual variability in the Amazon hydrologic cycle. J Geophys Res 104: 9097–9106

Zhang Y, Wallace JM, Battisti D (1997) ENSO-like interdecadal variability: 1900–93. J Climate 10: 1004–1020

Zhou J, Lau KM (2001) Principal modes of interannual and decadal variability of summer rainfall over South America. Int J Climatol 21: 1623–1644

Author's address: Jose A. Marengo (e-mail: marengo@cptec.inpe.br), Centro de Previsão de Tempo e Estudos Climaticos, CPTEC/INPE, Rodovia Dutra km 40, 12630-000 Cachoeira Paulista, São Paulo, Brazil.